Dynamics of orientationally disordered mixed crystal sharing Cl-adamantane and CN-adamantane

ARTICLE *in* JOURNAL OF NON-CRYSTALLINE SOLIDS · APRIL 2010

Impact Factor: 1.77 · DOI: 10.1016/j.jnoncrysol.2009.04.075

α-relaxation dynamics of orientanionally disordered mixed crystals composed of Cl-adamantane and CN-adamantane

J. C. Martinez-Garcia,[1] J. Ll. Tamarit,[1,a)] S. Capaccioli,[2] M. Barrio,[1] N. Veglio,[1] and L. C. Pardo[1]
[1]*Departament de Física i Enginyeria Nuclear, Grup de Caracterització de Materials, ETSEIB, Diagonal 647, Universitat Politècnica de Catalunya, 08028 Barcelona, Spain*
[2]*Dipartimento di Fisica, Università di Pisa and CNR-IPCF, Largo B. Pontecorvo 3, I-56127 Pisa, Italy*

(Received 21 October 2009; accepted 29 March 2010; published online 29 April 2010)

The α-relaxation dynamics of 1-cyano-adamantane (CNA) and its mixtures with 1-chloro-adamantane (ClA) has been studied by means of broadband dielectric spectroscopy. The existence of orientationally disordered (OD) face centered cubic mixed crystals ($ClA_{1-X}CNA_X$) for $0.5 \leq X \leq 1$ has been put in evidence by thermodynamics and structural analyses. In addition to the OD phase of CNA, mixed crystals with compositions higher than the equimolar one exhibit a freezing of the orientational degrees of freedom into a glassy state, which involves also a strong increase of the antiferroelectric order at temperatures higher than the dielectric glass transition temperature. This experimental evidence is revealed by a stairlike effect in the variation of the Kirkwood factor with the temperature as a consequence of a twin effect in the dielectric strength without any anomaly in the temperature-density curves. The characteristic relaxation times are analyzed as a function of temperature and mole fraction. By setting a common temporal origin ("isochronal origin") at $\tau(T_g)=100$ s for each mole fraction, it emerges that the substitution of ClA molecules by those of CNA (diminution of X) gives rise to a slow down in the dynamics, despite that the molecular volume of ClA molecules are smaller than those of CNA. This fact goes along and is accompanied by a diminution of the lattice packing with the decrease of composition. It is also shown that the heterogeneities produced by the concentration fluctuations due to the chemical disorder are the main contribution to the non-exponential character of the α-relaxation peaks. © *2010 American Institute of Physics*. [doi:10.1063/1.3397997]

I. INTRODUCTION

The dynamics of amorphous systems is one of the areas of great interest and challenging studies in the field of condensed matter physics.[1–4] From a general point of view, glass transition phenomenon appears when a dynamically disordered system, irrespective to the type of disorder, freezes by cooling or by pressuring. The freezing concerns atoms or molecules, the entities displaying some kind of disorder related to one or more degrees of freedom, in such a way that the entities slow down the dynamic properties until the glass transition (temperature or pressure laboratory glass transition) occurs. The slowing down process of one or more degrees of freedom of the entities is accompanied then by a rapid increase of viscosity or relaxation times associated with the primary (α-) relaxation of all kinds of physical macroscopic and microscopic observables, in such a way that, at the glass transition temperature, the frozen disorder scales with the time scale of the experiment (generally defined to be 100 s). The interactions and the cooperativity between the entities of the glass-forming material make the phenomenon a nontrivial many-body irreversible process.[1,5]

Despite the fact that there is no consensus on the most fundamental and universal behavior of this phenomenon, several theoretical approaches have been proposed to describe the specific behavior of glass formation.[6–8] At present, none of them can account for the dynamic heterogeneity that appears during the freezing process. The emergence of dynamic heterogeneities, i.e., superposition of intrinsically different exponential processes with different characteristic times, was first taken into account in the Adam–Gibbs approach,[6] based on cooperatively rearranged regions which increase the cooperativity during glass formation. However, although postulated long time ago, the existence of such cooperative rearranging regions or dynamical heterogeneities (i.e., domains of the liquid whose relaxation is highly correlated) has been only recently observed and identified in viscous liquids and polymers.[9–12] More recently, approaches based on the definition of dynamically correlated domains proposed the use of a four-point correlation function in order to quantify the size of growing length scale in supercooled systems occurring in vicinity of the glass transition that should be responsible for the increase of viscosity or/and relaxation time.[13–15] Because a theory providing insight into the microscopic origin of dynamic heterogeneity is still lacking, many (experimental and simulation) works focus on such a problem by characterizing the dynamics of monocomponent systems for which dynamics is analyzed throughout

a)Author to whom correspondence should be addressed. Tel.: +34 934016564. FAX +34 93 4011839. Electronic mail: jose.luis.tamarit@upc.edu.

the change of temperature and/or, sporadically, pressure. Fine tuning of these thermodynamic variables changes the intermolecular interactions between the particles of the system and thus the landscape dynamics. Another way to change the molecular surrounding of a relaxing entity and thus of the involved cooperativity, consists on mixing.[16–19] As compared to neat systems, binary glass formers so far have been studied to a lesser extent. In particular, so far the studies on binary mixtures are mainly (i) generally concerning a compound formed by molecules displaying a dipole moment and a second component devoid of static dipole or with a low dipole moment, in such a way that the dynamics of the former can be selectively monitored by means of a commonly used technique as dielectric spectroscopy, and (ii) focused on the increase of viscosity and the glass formation of supercooled liquids (structural glasses).

For canonical glass formers, i.e., those obtained from the liquid state, the freezing of dynamics concerns both translational and orientational degrees of freedom. On the contrary, for orientationally disordered phases, also called plastic phases, the center of mass of the entities are translationally ordered in a high-symmetry lattice while more or less free overall tumbling is present, in such a way that only orientational degrees of freedom are frozen at the glass transition, giving rise to a glassy crystal or OG.

Most plastic crystals are formed by molecules of more or less globular shape, providing in general little steric hindrance for reorientational processes. Among the substances displaying an orientationally disordered (OD) phase, the adamantane derivatives form a large and interesting group.[20–25] The pseudoglobular molecular shape of these compounds together with the dipolar character of the derivatives inferred by the substitution of one hydrogen in the adamantane molecule provides to this group interesting properties which can be used for fine tuning the required properties. In particular, several properties are known as relevant to make interesting these compounds.[22,26–28] On the one hand, overall free tumbling is impossible due to the hindering produced by the strong dipolar character for molecules with C_{3v} symmetry as for 1-X-adamantane substituted compounds $(X=Cl,Br,CN,\ldots)$.[29,30] On the second hand, fast rotations around the dipolar C_{3v} axis have been characterized to be faster than those concerning the overall molecular rotation, both being then clearly decoupled.[30,31] And, finally, these molecules are rigid and non-hydrogen bonded, so then secondary relaxations, if present, should be uniquely related to "pure" Johari–Goldstein β relaxations.[31]

The purpose of this paper is to investigate the dynamics of OD phases and, more into details, OD mixed crystals. The experimental two-component system is composed by two adamantane derivatives, Cl-adamantane (ClA) and CN-adamantane (CNA). Both molecules are known to be rigid, within the spatial range we are concerned, with a C_{3v} molecular symmetry and dipole moments along their threefold axis.[32,33] Thus intramolecular motions of some subgroup dynamically decoupled from the rest of the molecule, giving rise to a secondary (β-) process in the dynamic behavior, are unlikely to occur in the experimentally investigated timescale range.[31] As for the bending motion of the C–C≡N group, Raman scattering measurements have shown that the characteristic frequency at room temperature is around 4.5 THz, so far away from the frequency domain of the present study.[34]

Although β-processes, faster than the α-process, due to local intermolecular motions (also called Johari–Goldstein processes) often observed for glass forming materials can appear, they will be out of the scope of the present work.[12] The main goal of the paper is the study of the effect of mixing on the cooperative α-relaxation leading to the glass transition.[35] The rest of the paper is organized as follows. Details of the experimental devices are given in Sec. II. Results obtained for each experimental technique can be found in Sec. III. Section IV is devoted to the discussion of the results by considering all the available experimental information. Finally, conclusions are gathered in the last section, Sec. V.

II. EXPERIMENTAL

A. Sample

Pure compounds 1-cyano-admantane, CNA, $(C_{10}H_{15}CN)$ and 1-chloro-adamantane ClA $(C_{10}H_{15}Cl)$ were purchased from Aldrich Chemical Co. with purity grades of 98% and used without additional purification because the transition and melting temperatures and enthalpy changes fully agreed with previous reported values.[22,26,36,37] Two-component mixed crystals, $ClA_{1-X}CNA_X$ with $0.50 \leq X \leq 1$, were prepared from the melt of the pure compounds in the selected proportions into screw-cap tubes by slow cooling to room temperature.

B. Experimental techniques

1. Differential thermal analysis

Differential thermal analysis were performed by means of a TA-Q100 from TA Instruments equipped with a RCS low-temperature adapter to determine melting temperatures and to check whether the transition temperatures to the low-temperature ordered phases or the supercooled character of the OD phases. Sample masses around 15 mg hermetically sealed into high-pressure stainless steel pans under He flux were measured using scanning rates of 2 K min^{-1}.

2. X-ray powder diffraction

High-resolution x-ray powder diffraction measurements using the Debye–Scherrer geometry and transmission mode were performed with a vertically mounted INEL cylindrical position-sensitive detector (CPS-120) made of 4096 channels (0.029° 2θ angular step).[38] Monochromatic Cu $K\alpha_1$ radiation (λ(Cu $K\alpha_1$)=1.5406 Å) radiation was selected by means of an asymmetrically focusing incident-beam curved quartz monochromator. The generator power was set to 35 kV and 35 mA. External calibration to convert the measured 4096 channels to 2θ degrees using $Na_2Ca_2Al_2F_4$ cubic phase was applied by means of a cubic spline fitting procedure.[39] The peak positions were determined after pseudo-Voigt fitting by using standard procedures. Details can be found in Refs. 40 and 41.

Measurements as a function of temperature in the temperature range of 100 K < T < 400 K were achieved with a liquid nitrogen 700 series Cryostream Cooler from Oxford Cryosystems. Powder samples were placed into Lindemann capillaries (0.3 inner diameter) at room temperature. During data collection, capillaries were rotated perpendicularly to the x-ray beam direction to minimize possible effects of preferred orientations.

3. Dielectric spectroscopy

Dielectric spectra were collected with an Alpha impedance analyzer (10^{-2}–10^{7} Hz) from Novocontrol. The special parallel-plate capacitor (diameter 5 mm) was filled in the plastic phase and electrodes were put separated by inserting several 50 μm silica spacers and submitted to a hand press. The temperature of the sample was controlled by a System Quatro from Novocontrol using a heated nitrogen gas stream.

The isothermal measurements as a function of the frequency were carried out above the glass transition temperatures on cooling as different steps (typically 5 K) with a temperature control of ±0.2 K. Each isothermal measurement started 15 min after temperature stabilization.

The real and imaginary part of the complex permittivity, $\varepsilon^*(\nu)=\varepsilon'(\nu)-i\varepsilon''(\nu)$, were described by using the well-known Havriliak–Negami equation plus the dc conductivity contribution,

$$\varepsilon^*(\nu)=\varepsilon'(\omega)-i\varepsilon''(\omega)=\varepsilon_\infty+\left\{\frac{\varepsilon_s-\varepsilon_\infty}{(1+(i2\pi\nu\tau_{HN})^{\alpha_{HN}})^{\beta_{HN}}}\right\}-i\frac{\sigma}{\varepsilon_o 2\pi\nu}, \quad (1)$$

where τ_{HN} is the relaxation time of the process, ε_s, ε_∞, and $\varepsilon_s-\varepsilon_\infty$ stand for the static permittivity, the asymptotic value of permittivity at high frequencies of the dielectric constant and the dielectric strength ($\Delta\varepsilon$), respectively, and α_{HN} and β_{HN} are the characteristic fractional shape parameters of the dielectric loss curve ($\alpha_{HN}\cdot\beta_{HN}$ for the high-frequency wing and α_{HN} for the low-frequency wing accounting for the asymmetric broadening with respect to the Debye behavior).

III. RESULTS

A. Pure compounds

CNA is a rigid cage molecule with a C≡N radical group which confers a strong dipolar moment (μ=3.83 D). The only internal degree of freedom corresponds to the motion of C–C≡N group, the associated dynamics being far away from the frequency range analyzed in this work.[31,34] This compound has been studied by means of an extended number of experimental techniques as dielectric spectroscopy, NMR, thermal analysis, inelastic x-ray scattering, calorimetry, thermally stimulated discharge currents, and Raman spectroscopy.[20–34,36,37,42] Some molecular dynamics studies have also been reported.[21,30] As far as its polymorphism is concerned, it has been clearly stated that the melt crystallizes into an OD cubic plastic phase with Fm3m symmetry at approximately 462 K.[33] This phase is dynamically characterized by restricted tumbling in such a way that six equilibrium orientations along the ⟨001⟩ directions can be distinguished, as well as threefold uniaxial rotations around the C–C≡N group, i.e., the C_{3v} axis corresponding to the dipolar molecular axis, which means that such disorder is not seen by dielectric spectroscopy.[32,33] At lower temperatures, CNA transforms to a more ordered crystalline phase, the structure of which is known to be monoclinic (space group C2/m) with an antiferroelectric order. In fact, the local antiferroelectric order in the OD phase is known to be reminiscent of such an order in the low-temperature monoclinic phase.[43] In this low-temperature ordered phase, the uniaxial rotations along C_{3v} axis also remain. The OD phase can be easily quenched by cooling into a glassy crystal, the nonergodic state associated with the ergodic OD phase, with a glass transition temperature at about 170 K.[36,43–46] As far as this glass transition is concerned, Yamamuro *et al.*[36] argued that in fact orientational degrees of freedom can be frozen in at higher temperatures and, in the recent work from Carpentier *et al.*,[25] this transition is much more related with the freezing of the fluctuations of an antiferroelectric local ordering, occurring on a size and time scale larger than those characteristic of the dynamic slowing down (i.e., $\tau(T_g)$=100 s). On further heating after the quenching process or simply aging at temperatures higher than T_g, the supercooled OD fcc phase transforms to the low-temperature ordered phase via an intermediate metastable phase.[25,47] Figure 1 depicts the lattice volume per molecule of the OD phase and of the nonergodic state, the orientational glass (OG) state. It clearly evidences the well-known change of the isobaric thermal expansion coefficient at the glass transition. It should be noticed that after the quenching at 100 K x-ray patterns as a function of the increasing temperature only showed Bragg reflections corresponding to the fcc lattice.

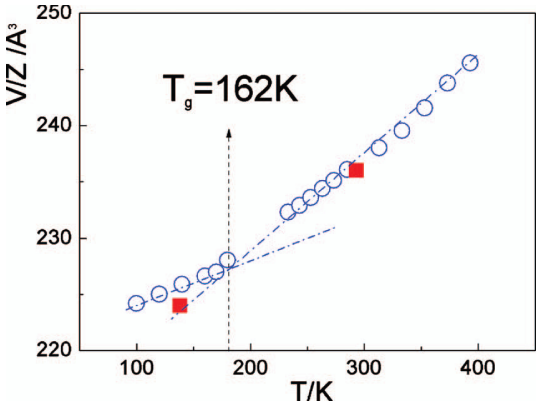

FIG. 1. Volume per unit of molecule of the OD fcc phase and the OG for the CNA on heating after quenched at 100 K from room temperature and on heating after cooling down until 233 K. The squares correspond to the values from Refs. 43 and 45.

Dielectric spectroscopy has proven to be an important tool for the investigation of the orientational dynamics in canonical glass formers as well as in plastic crystals. For both cases, the dielectric spectra are dominated by the α-relaxation process, showing up as a peak in the frequency-dependent dielectric loss, with the ubiquitous requirement of the dipolar character of the relaxing entity. The dynamics of the OD of CNA has been studied in detail by means of dielectric spectroscopy and NMR.[20,25,31,44,45,48]

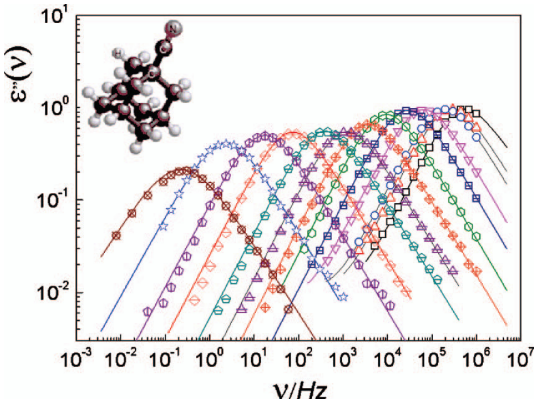

FIG. 2. Double logarithmic representation of selected dielectric loss spectra of CNA from 293 to 173 K (measurements were performed every 5 K, but we show only one over two for clarity). The lines show the fits using the HN function for the α-relaxation processes. Inset shows the molecular structure of CNA.

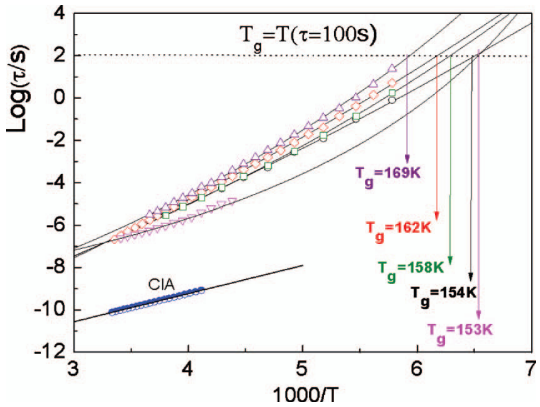

FIG. 3. Arrhenius plot of the α-relaxation time vs inverse temperature for the pure compound CNA (black circles) and various ClA_{1-X} CNA_X mixed crystals, X=0.80 (red diamonds), X=0.69 (green squares), X=0.62 (violet triangles), and X=0.5 (pink inverted triangles). Values for ClA (blue circles) were calculated according to the data provided by Amoureux *et al.* (Ref. 51).

Figure 2 shows the dielectric loss spectra for various selected temperatures on cooling from room temperature obtained in this work. For all the studied temperatures, a single peak is observed, although the full width at half maximum clearly exceeds that of the monodispersive Debye relaxation process. The α-relaxation peaks in imaginary part of dielectric permittivity also exhibit an asymmetric broadening: for this reason they were fitted according to the empirical Havriliak–Negami equation [Eq. (1)]. For temperatures lower than approximately 235 K, the dielectric strength diminishes due to the onset of an antiferroelectric arrangement of molecular dipoles as we will see through the analysis of the Kirkwood factor. As for the latter, it has been recently argued[45] that the glass transition for CNA is strongly related with the freezing of fluctuations of an antiferroelectric local ordering, which gives rise to a diminution of the permittivity strength at low temperatures on approaching the glass transition, an effect that was already postulated in the pioneering work of Amoureux *et al.*[45] This ordering process was highlighted by the analysis of the appearance of diffuse scattering spots at the X-boundary points of the Brillouin zone as a consequence of a emergence of local ordering close to the glass transition temperature.[25]

Studies on plastic crystals showed that the shift of the primary α-relaxation on cooling can be well represented by the Vogel–Fulcher–Tammann (VFT) dependence, namely

$$\tau(T) = \tau_0^{\mathrm{VFT}} \exp\left[\frac{D_T T_0}{T - T_0}\right], \tag{2}$$

where the temperature T_0 is an estimation of the ideal glass transition, also called the Vogel–Fulcher temperature) and D_T is the strength parameter which is anticorrelated with the fragility (m) of the material for the given temperature domain.[49,50] The Arrhenius plot of the primary (α) dielectric relaxation time in the supercooled OD phase for CNA is depicted in Fig. 3. The relatively high value (in the range 50–140, see also Fig. 8) of the strength parameter (as far as OD phases is concerned) together with a very low value of T_0 brings the temperature dependence of timescale [Eq. (2)] to have a behavior very similar to an Arrhenius one and that indicates, within the strong-fragile classification scheme by Angell,[52] the strong character of this OG, a result generally observed for many of this class of materials, although relevant exceptions have been found.[53]

The OD fcc phase (Fm3m space group symmetry) of ClA (μ=2.39 D) (Ref. 54) ranges from 249 K until the melting point at ca. 439 K.[22] As for the case of CNA, ClA molecule undergoes reorientational movements of its C_{3v} molecular axis between the fourfold crystallographic axes together with fast uniaxial rotations about the C_{3v} molecular axis. In addition, it has been found that first- and second-nearest neighbors have strong dipole-dipole correlation that gives rise to a noticeable short-range order (ferroelectric or antiferroelectric order).[51,55] Such a strong correlation produces a rather restricted reorientation of ClA molecules as compared to the expected from the symmetry of the space group Fm3m. Dielectric studies have demonstrated that the order is clearly antiferroelectric as evidenced by the low value of the Kirkwood factor (ranged between 0.8 close to the melting temperature and 0.3 close to the transition temperature).[51] Although molecular dynamics simulations[21] claim for the existence of a OG ($T_g \approx 217$ K), as far as we know, no experimental evidence has been published till now. Dielectric spectroscopy results indicate also that the dynamics of the ClA molecules in the OD phase is very fast, with reorientational times faster than approximately 1 ns (at around 245 K).[51] At temperatures below the OD phase, ClA transforms to a low-temperature ordered phase (monoclinic $P2_1/c$, Z=4) in which the fast uniaxial rotations remain.[22]

B. Mixed crystals

In order to analyze the influence on the dynamics of the molecular substitution in the CNA OD lattice of similar dipolar molecules (ClA), OD mixed crystals between both compounds have been characterized. The formation of OD mixed crystals (solid solutions of substitutional type) was studied in the concentration range $0.50 \leq X < 1$ and controlled by means of differential thermal analysis and high-resolution x-ray powder diffraction. As for the calorimetric

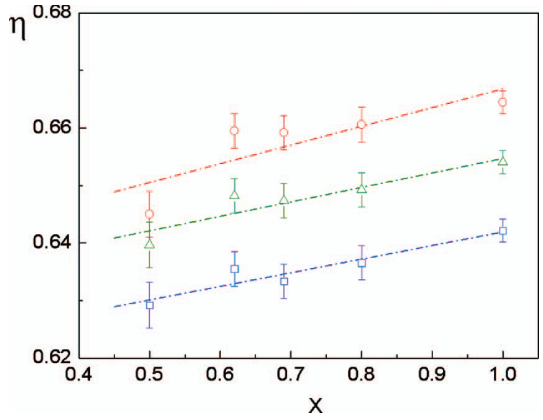

FIG. 4. Packing coefficient of the OD fcc $(ClA)_{1-X}(CNA)_X$ mixed crystals as a function of the mole fraction at several temperatures: 178 K (circles), 233 K (triangles), and 288 K (squares). Lines are guides for the eyes.

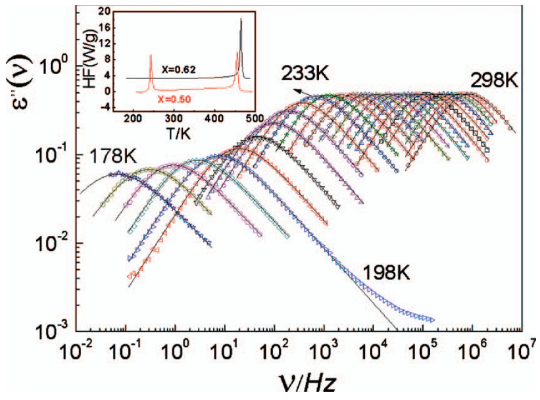

FIG. 5. Double logarithmic representation of selected dielectric loss spectra of $(ClA)_{0.38}(CNA)_{0.62}$ mixed crystal in the OD fcc phase at various temperatures. Solid curves are the fitting function described by Eq. (1). The dielectric loss at T=198 K is shown for the whole frequency range to highlight the existence of an excess wing (see text). The inset shows the DSC measurements for mixed crystal $ClA_{0.38}CNA_{0.62}$ (black) and $ClA_{0.50}CNA_{0.50}$ (red).

technique, for compositions with mole fraction higher than 0.5, only one melting peak was found, which means that the OD phase of the mixed crystals does not transform to a more ordered structure (see inset in Fig. 5). To guarantee the existence of a unique OD fcc phase in the concentration domain, i.e., to establish the isomorphism relationship between the OD phases of pure compounds,[41] x-ray diffraction was undertaken as a function of temperature for each composition. Both thermal and x-ray diffraction measurements clearly establish the existence of OD fcc mixed crystals for the studied concentration range, which demonstrates the isomorphism relationship between both OD fcc phases of pure compounds. It should be pointed out that even for low temperatures all the Bragg reflections of the patterns were fully indexed within the fcc symmetry and no additional reflection concerning the appearance of an additional more ordered structure appeared. The only exception concerns the equimolar mixed crystal for which a phase transition was detected around 230 K (see inset in Fig. 5). A simple tool to obtain information about the intermolecular interaction is the use of the packing coefficient (η). This approach consists of comparing the volume of the molecules (V_m) with the available volume in the lattice (V/Z), where V is the unit-cell volume and Z the number of molecules in the unit cell ($Z=4$ for a fcc lattice). Thus, the packing coefficient is defined as the ratio $V_m/(V/Z)$. According to this definition, the packing variation as a function of the composition and temperature can be determined as $\eta(X,T)=V_m(X)/(V(X,T)/Z)$. The available volume $V(X,T)/Z$ is straightforwardly calculated from the lattice parameters obtained from the x-ray pattern refinements. The simplest way to calculate $V_m(X)$ is to set the average of the volumes of the isolated rigid and nonhydrogen bonded molecules shared in the mixed crystal, i.e., $V_m(X)=(1-X)V_m(ClA)+XV_m(CNA)$.[56] The molecular volumes of the pure components, computed using the values of the van der Waals radii and interatomic chemical bonds following Kitaigorodsky's method,[57] were determined to be 149.05 and 152.00 $Å^3$ for ClA and CNA, respectively. Reference van der Waals radii and interatomic chemical bonds were taking from Ref. 58.

Figure 4 gives the variation of the packing coefficient as a function of mole fraction of CNA for three temperatures. As can be seen from the figure, packing coefficient increases with the mole fraction (although that molecular volume of the CNA molecule is larger than that of the ClA). It means then that substitution of CNA molecules does produce a reinforcement of the intermolecular interactions, in spite of the close similarity between both molecular entities. This experimental finding agrees, as we will see later when analyzing the Kirkwood factor as well as the dynamics as a function of mole fraction, with the increase of the antiferroelectric ordering and the cooperativity with the increase of CNA content.

OD mixed crystals were also characterized by means of dielectric spectroscopy. Selected dielectric loss spectra corresponding to the $(ClA)_{0.38}(CNA)_{0.62}$ mixed crystal are presented in Fig. 5, showing the α-relaxation process. None of our systems (including the pure CNA compound and all the mixtures) presents an excess wing or a secondary peak in the frequency and temperature range of interest for this work. Nevertheless, it should be noticed that for the low-temperature domain of mixtures an excess wing shows up at the high frequency flank of the α-peak (see the dielectric loss at T=198 K in Fig. 5). Such a deviation from the asymptotic power law behavior of the α-peak, interpreted as an excess wing was detected also for CNA by Brand *et al.*[59] but it could be also compatible with the secondary relaxation identified by Pathmanathan and Johari[31] at very low temperature and high frequencies with an strength of around 500 times smaller that the main α-relaxation.

Due to such a small strength and to the great frequency separation from the α-process, the authors attributed this process to a few number of localized configuration states (localized regions due to spatial heterogeneities giving rise to a Johari–Goldstein relaxation) ruling then out the possible existence of such a secondary relaxation for all the molecules.

Due to the cooperative character of the α-relaxation process, there is no doubt that molecules of both types participate together into the same α-relaxation process. Thus, a unique Havriliak–Negami equation was used to account for the dielectric losses. From that, the relaxation time of the

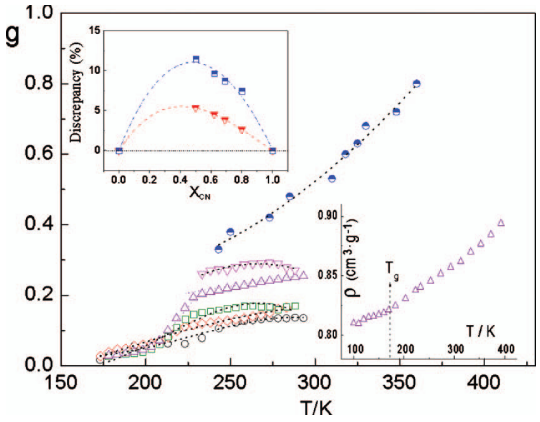

FIG. 6. Kirkwood factor as a function of temperature for several mole fractions (symbols as in Fig. 3). Values for ClA (open circles) were obtained from Amoureux *et al.* (Ref. 51). The upper inset shows the relative deviation from the calculation of g used in the main plot from the values obtained according two other procedures described in Refs. 61 and 62. The lower inset shows the density as a function of temperature for the $ClA_{0.38}CNA_{0.62}$ mixed crystal.

maximum of the loss peak for each composition as a function of temperature was obtained: they are plotted in the Arrhenius diagram of Fig. 3. A first and overall inspection of Fig. 3 seems to indicate that for mole fractions higher than 0.5, at a given temperature, the dynamics is slowed down when molecules of CNA are substituted by those of ClA, i.e., with decreasing the mole fraction X of CNA. This is, at least, a very surprising phenomenon when dynamics of pure compounds is recalled, because for the OD phase of ClA dynamics concerning the overall molecular tumbling is several orders of magnitude faster than that of the CNA at the same temperature.[51]

IV. DISCUSSION

The existence of miscibility in the OD fcc phase evidenced by thermal and x-ray powder diffraction measurements has enabled us to determine the volume of the cubic unit-cell and thus, the density as a function of the temperature and of the mole fraction. Owing to the cubic symmetry (spatial isotropy), the Kirkwood–Frölich theory[60] accounts for the local order through the Kirkwood factor, g, which can be expressed by

$$g = \frac{9k_BT}{4\pi\mu^2}\frac{V}{N}\frac{(2\varepsilon_s+\varepsilon_\infty)(\varepsilon_s-\varepsilon_\infty)}{\varepsilon_s(2+\varepsilon_\infty)^2}, \quad (3)$$

where k_B is the Boltzmann constant, μ is the dipole moment of the molecular entity, and V/N stands for the reciprocal of the number of dipoles per unit volume. For mixtures, usually the g factor is obtained by using an equation similar to the above mentioned equation, but with μ indicating an effective dipole moment, calculated from a combination of the dipole moments of the different molecular species, weighted according to different methods.

Figure 6 shows the variation of the Kirkwood g factor as a function of temperature for pure compounds and several mixed crystals in the OD fcc phase. As far as the effective dipole moment μ of the molecular entity, it has been calculated for the mixtures following the procedure of the molecular volume for the packing coefficient, i.e., as a linear combination of the square dipole moment for the pure compounds with the mole fraction.[63,64] It is noteworthy to point out that if calculation of effective μ^2 is performed according to other methods, like for instance weighting the square dipoles by volume fractions or by mass fractions[60,65–67] the trends are exactly the same and only an small shift, with a discrepancy less than 10%, on the Kirkwood factor is observed (see upper inset in Fig. 6).[61,62,64]

It should be noticed that g values for CNA are slightly different from those previously published,[51] probably because those authors kept the density constant (1.13 g cm^{-3}) for the whole temperature domain in their calculations.

For the analyzed pure compounds and mixed crystals, three straightforward results from the g factor are evidenced: (i) it is always smaller than unit; (ii) it decreases with increasing the mole fraction of CNA; and (iii) it increases with temperature. As for the first experimental finding, it means that short-range correlations orient dipole entities in a strong antiferroelectric order. As for the second, the results coherently support the fact that the packing coefficient (see Fig. 4) increases with the mole fraction of CNA giving then rise to an increase of the steric hindrance of the molecular reorientation. And, as for the last, it simply makes evident the increase of thermal expansion with temperature yielding to a softening of the thermal vibrations going along with a small increase of the ε_s. Nevertheless, it should be mentioned that the stairlike behavior of g for some mixtures is a direct consequence of the changes of the permittivity strength as a function of temperature (see Fig. 5 for X=0.62) and it is not related to a change in the density (see the lower inset in Fig. 6 showing the continuous variation of density). This effect points out a rapid development on cooling of a local arrangement of molecular dipoles that should be attributed to a strong increase of the antiferroelectric order at temperatures higher than the corresponding glass transition temperature, in good agreement with what recently found in pure CNA.[25]

According to Fig. 3 the relaxation time for the α-process becomes longer, for a given temperature, when molecules of CNA are substituted by those of ClA, i.e., with decreasing the mole fraction X (with the exception of the equimolar composition). Nevertheless, such an Arrhenius plot lacks of the pertinent normalization of the temperature axis, because, in order to see how mixing can affect the intermolecular coupling and cooperativity, dynamics should be renormalized for the whole temperature range with respect to a common "origin." The well-known Angell plot enables such a rescaling in a natural way with the common origin at T_g, where the relaxation time is assumed to be 100 s, ensuring thus a reference state (the glass transition temperature) for each sample with the same *isochronal state*. Figure 7 shows the relaxation times as a function of the renormalized temperature variable, $u=T_g/T$, i.e., the so-called Angell plot.[68] It can be inferred that, within the frame of the T_g/T reduced variable, the dynamics for all mixed crystals appears according to a physically meaningful and coherent scenario. The picture means that the introduction of the smallest molecules of ClA with a lower dipole moment into the lattice of the

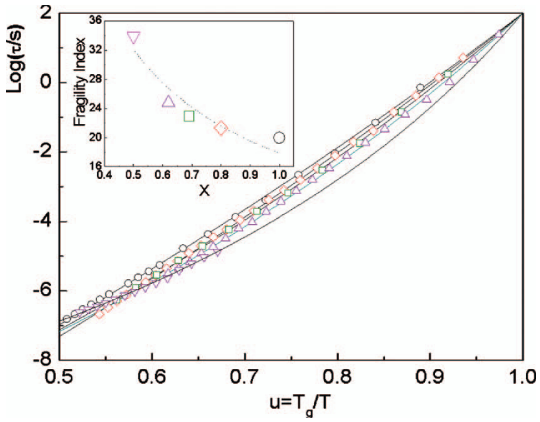

FIG. 7. The Angell plot showing the relaxation time (log scale) as a function of inverse temperature normalized to the dielectric glass transition temperature T_g. The inset shows the fragility as a function of the mole fraction (symbols as in Fig. 3).

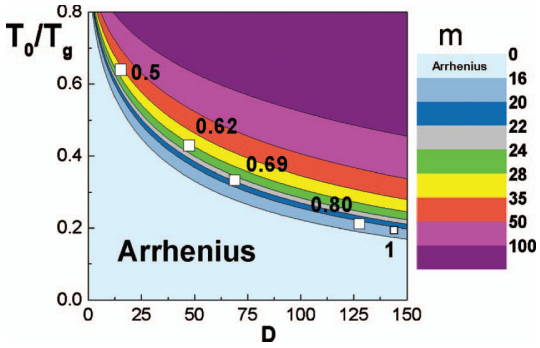

FIG. 8. 3D plot of Eq. (5) as a function of T_0/T_g, D, and m variables.

CNA molecules is a process which goes with a decrease of the packing coefficient (see Fig. 4) and with a shortening of the relaxation time, i.e., the reorientation becomes faster for the average molecular entity. In addition, the substitution process of CNA molecules by ClA molecules (i.e., a decrease of the mole fraction) increases the Kirkwood factor (Fig. 6) giving then rise to a diminution of the strong antiferroelectric order shown by the OD phase of CNA, reinforcing then the conclusions obtained from Carpentier *et al.*[25]

Another evidence of the coherence between Kirkwood factor results and dynamics data found for the mixed crystals can be obtained from the fragility parameter m (see inset of Fig. 7). The non-Arrhenius behavior of relaxation time is described commonly according to the Angell's fragility,

$$m(x) = \left(\frac{\partial \log_{10} \tau(T,x)}{\partial (T_g/T)} \right)_{T=T_g(x)}, \tag{4}$$

which indicates the steepness of the evolution of the relaxation time (or viscosity) as a function of T near to T_g for each mole fraction. It ranges from a lowest limiting value of 16 for strong glasses to values as large as 191 for very fragile glasses as poly(vinyl chloride).[69] In the present case the fragility parameter m ranges between 20 (CNA) and 34(X =0.50) with a clear decreasing trend as a function of mole fraction of CNA.

The value of fragility parameter m can be subjected to big discrepancies, depending on the method used to calculate it. The most popular method is to obtain it from the analysis of the parameters of Eq. (2), mostly determined from data far away from T_g and so affected by big uncertainties. If the fitting procedure of the dynamics data is not correctly provided, usually the ratio T_0/T_g and D are not anticorrelated and the prefactor τ_0^{VFT} attains to unreasonable small or large values.[70] The exact relation between fragility m and strength coefficient D introduced in Eq. (2) can be derived as

$$m(x) = \frac{D(x)}{\ln 10} \frac{T_0(x)/T_g(x)}{(1-(T_0(x)/T_g(x)))^2}, \tag{5}$$

where the dependence on the mole fraction has been made explicit.

Figure 8 shows the coherence between the dynamic values obtained for each mixed crystal. It nicely evidences the increase of the strength parameter D when the mole fraction of CNA decreases together with a continuous and coherent change of the T_0/T_g ratio. One should be aware that values for $ClA_{0.50}CNA_{0.50}$ mixed crystal were obtained from the fitting of relaxation times clearly far away from the extrapolated T_g, so this extrapolation must be considered as a rough approximation. In spite of that, results for such a composition are coherently located within the framework.

The increase of fragility with the substitution of CNA molecules with ClA molecules (decrease of the mole fraction X in inset of Fig. 7) and the consequent increase of cooperativity and timescale of the α-relaxation could be rationalized in term of frustration based approaches.[71] "Frustration" in that context describes an incompatibility between extension of the local order preferred in a molecular system and tiling of the whole space. From the scaling argument analysis, Tarjus and co-workers found that "one can associate a large fragility with a small frustration." Indeed, on decreasing CNA mole fraction, the antiferromagnetic order decreases and the system becomes more fragile.

The shape parameters α_{HN} and β_{HN} [Eq. (1)] of the α-relaxation have been determined from the fit of HN function. The former is close to 1 in the high-temperature domain whatever the composition is, which means, as observed in other OD phases, that the Cole–Davison function can accurately describe the non-Debye relaxation process. As far as β_{HN} parameter is concerned, it is almost temperature independent but strongly dependent on composition of the mixed crystal. Approaching the glass transition temperature, the common feature of many glass-forming materials, i.e., a decrease of the shape parameters with temperature, is found, indicating the strong deviation from the Debye behavior commonly attributed to the increase of temporal and spatial heterogeneities.

Another way to describe the relaxation corresponds to the Kohlrausch–Williams–Watts (KWW) stretched relaxation function,[72,73]

$$\varphi(t) \propto \exp[-(t/\tau)^{\beta_{KWW}}], \tag{6}$$

where β_{KWW} is the stretched parameter. Experimental dielectric spectra, obtained in the frequency domain, were transformed to the time domain through the use of the connection between dielectric permittivity and relaxation function via

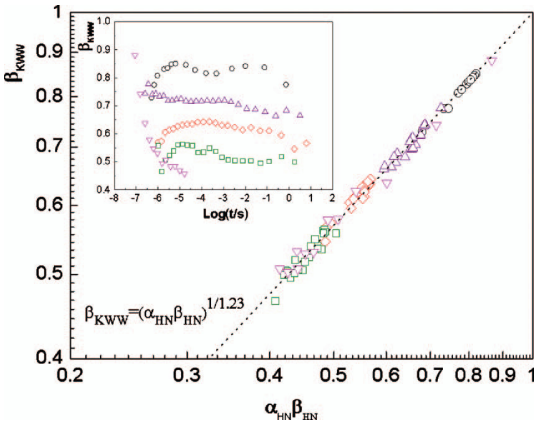

FIG. 9. Double logarithmic scale for the β_{KWW} stretched exponent of the KWW relaxation function as a function of the shape parameters α_{HN} and β_{HN} of the Havriliak-Negami expression [Eq. (1)]. Dashed line corresponds to the relationship between β_{KWW} and α_{HN} and β_{HN} shape parameters provided by Alegria *et al.* (Ref. 74).

the Laplace transformation and β_{KWW} stretched parameter was directly fitted for each temperature and mole fraction. Figure 9 shows the relationship between such a fit parameter and those obtained from the fits of the HN equation. It is evidenced that the proposed relation for structural glasses from Alegria *et al.*[74] $(\alpha_{HN}\cdot\beta_{HN})^{1/1.23}$(dashed line in Fig. 9) perfectly works for the whole temperature and composition studied range. It is also seen at a first glance that the dielectric relaxation process becomes highly nonexponential when increasing the dilution of CNA with ClA molecules (decrease of the mole fraction). Moreover, the nonexponential character is strongly dependent on composition and noticeably stronger on increasing the relaxation time (see inset in Fig. 9). This result shows that local heterogeneities generated by the compositional disorder control the relaxation process, a result which is similar to that previously found for structural glasses.[75] Local concentration fluctuations can broaden the loss peaks well above than what expected for a variation of intermolecular interactions. For the mixed crystal $ClA_{0.38}CNA_{0.62}$, the distribution of the relaxation times appears to be sharper when compared to the observed general behavior of mixed crystals. Although it is difficult to establish a physical reason for such a result, it is clear that some kind of special short-range order appears for this composition making the dynamic behavior closer to that of CNA pure compound as far as the distribution of the relaxation times is concerned.

In order to ensure the relevance of the described chemical disorder induced by compositional changes, the influence of the density has been analyzed. Normalized dielectric relaxation spectra for some selected common values of relaxation time τ (a), T_g/T value (b) and density (c) are displayed in Fig. 10. The broadness of the α-relaxation process varies between that of the CNA pure compound and that of the $ClA_{0.31}CNA_{0.69}$, whatever the physical parameter is used for comparison and it is exclusively dependent on concentration. Thus, the nonexponential character evidenced by the broadening of the α-relaxation peak and characterized by the β_{KWW} stretched parameter is caused by the heterogeneities

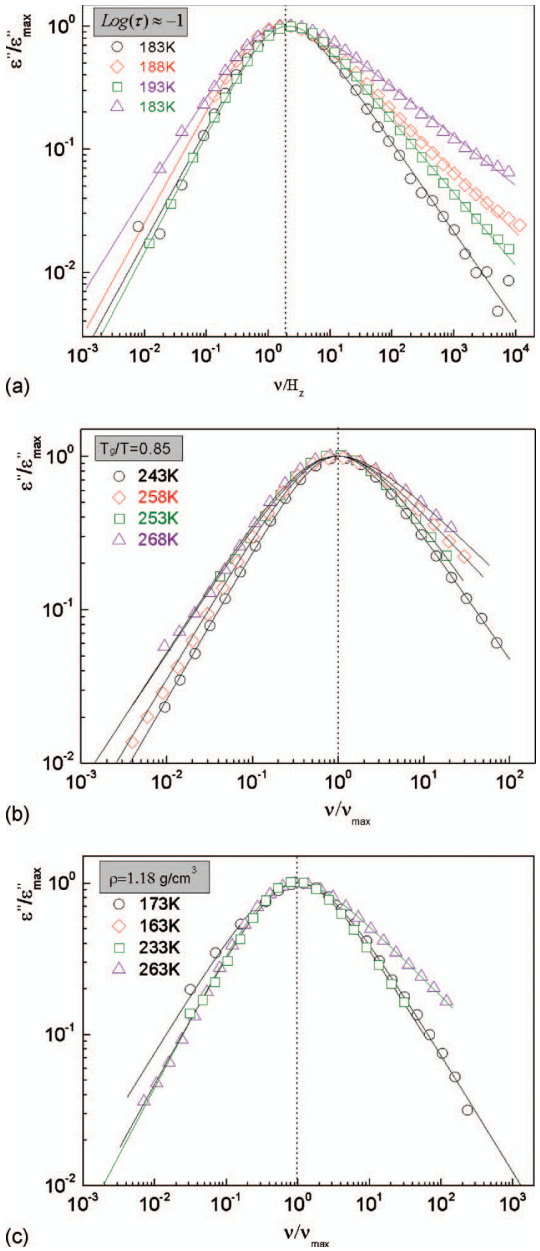

FIG. 10. Normalized dielectric spectra for some selected common values of relaxation time log $\tau=-1$ (a), reduced temperature $T_g/T=0.85$ (b), and density of 1.18 g cm^{-3} (c) for the mixed crystals $ClA_{1-x}CNA_x$.

produced by the concentration fluctuations which are the consequence of a statistic (chemical or compositional) disorder and not induced by dynamic correlations. Nevertheless, the special findings found for the $ClA_{0.38}CNA_{0.62}$ mixed crystal suggest that particular spatial short-range ordering can give rise to a sharper distribution of the relaxation time. Although to substantiate this claim inelastic neutron scattering should be performed in order to correlate both structure and dynamics, the Kirkwood factor (Fig. 6) offers already some hints of a related behavior. For both CNA and ClA the relaxation process involves the tumbling motion of molecules in an antiferroelectric local ordering, the character of which increases with the increase, in the lattice, of CNA molecules, bearing a strong dipole moment. Nevertheless,

the mixed crystal deserving the special behavior, $ClA_{0.38}CNA_{0.62}$, falls out of the general trend and the g factor is closer to that of ClA than to that of CNA, making evident that the antiferroelectric ordering, although still high, is lower than the value expected according to the trend of the other analyzed mixed crystals.

Finally, it is worth to emphasize that OD phases giving rise to glassy states present many peculiarities and fail to obey some general trends found for structural glasses. Among them, the well-known correlation between the fragility and the β_{KWW} stretched parameter found by Böhmer *et al.*[69] $m=(250\pm30)-320\cdot\beta_{KWW}(T_g)$. β_{KWW} parameter ranges between 0.75 and 0.50 close to T_g (as inset in Fig. 9 shows), while the variation of fragility (see inset in Fig. 7) changes between 20 and 34. Actually, the Böhmer's relation works, within the limit error, for pure compound CNA, but fails for mixed crystals in such a way that with increasing the mole fraction m increases and accordingly, $\beta_{KWW}(T_g)$ decreases but this decrease being much faster due to the concentration fluctuations and compositional disorder.

V. CONCLUSIONS

The existence of OD mixed crystals between ClA and CNA has been put in evidence by means of thermal and x-ray diffraction measurements. The dynamics of the α relaxation process corresponding to the molecular tumbling of molecules in the fcc lattice of the pure compound CNA and the OD mixed crystals $ClA_{1-X}CNA_X$ for $0.50\leq X\leq 1$ has been studied through dielectric spectroscopy.

The results concerning the variation of the Kirkwood factor evidence a strong antiferroelectric order of molecular entities, which increases with the mole fraction of CNA and with the decreasing of temperature. In addition, for all the compositions higher than 0.5 and even for CNA pure compound, a stair-like diminution is observed between 220 and 240 K as a consequence of the reinforcement of an antiferroelectric ordering. Such a change comes from an abrupt diminution of the dielectric strength together with a continuous variation of density as a function of temperature.

As for the relaxation times, in addition to the ubiquitous diminution when approaching the glass transition temperature for each mixed crystal, they increase with the increase of the ClA molecules (with small molecular volume and dipole moment) in the lattice. This experimental evidence can only be rationalized when relaxation times are analyzed in the framework of the Angell plot, i.e., when the temperature variable is normalized according to a common "dynamic" origin for all the analyzed compositions (an "isochronal" origin at $\tau(T_g)=100$ s). In addition, such a substitution process of CNA molecules, by those of ClA giving rise to a faster dynamic behavior, is coherently accompanied with a decrease of the packing coefficient. This indicates that the steric repulsions between the van der Waals envelopes of the involved molecular entities determine significantly the strong orientational short-range order, which at low temperatures gives rise to an antiferroelectric arrangement of the entities. Actually, less strong are the involved dipole moments and the intermolecular potential, weaker is the antiferroelectric order.

Finally, the nonexponential character evidenced by the broadening of the α-relaxation peak and characterized by the β_{KWW} stretched parameter with the diminution of the mole fraction is caused by the heterogeneities produced by the concentration fluctuations which are the consequence of a statistic (chemical) disorder and not induced by dynamic correlations.

ACKNOWLEDGMENTS

This work was supported by the Ministry of Science and Innovation through Grant No. FIS2008-00837 and by the Catalonia Research Ministry through Grant No. 2009 SGR 1251. One of us (J.C.M.G.) acknowledges the Ph.D. fellowship from UPC. The authors wish to thank Dr. P. Negrier for calculation of the molecular volumes for ClA and CNA.

[1] P. G. Debenedetti and F. H. Stillinger, Nature (London) **410**, 259 (2001).
[2] C. A. Angell, K. L. Ngai, G. B. McKenna, P. F. McMillan, and S. W. Martin, J. Appl. Phys. **88**, 3113 (2000).
[3] K. L. Ngai, J. Non-Cryst. Solids **353**, 709 (2007).
[4] P. Lunkenheimer, U. Schneider, R. Brand, and A. Loidl, Contemp. Phys. **41**, 15 (2000).
[5] H. Shintani and H. Tanaka, Nat. Phys. **2**, 200 (2006).
[6] G. Adam and J. H. Gibbs, J. Chem. Phys. **43**, 139 (1965).
[7] W. Götze and L. Sjögren, Rep. Prog. Phys. **55**, 241 (1992).
[8] K. L. Ngai, J. Phys.: Condens. Matter **15**, S1107 (2003).
[9] M. D. Ediger, Annu. Rev. Phys. Chem. **51**, 99 (2000).
[10] H. Sillescu, J. Non-Cryst. Solids **243**, 81 (1999).
[11] R. Richert, J. Phys.: Condens. Matter **14**, 201 (2002).
[12] U. Tracht, M. Wilhelm, A. Heuer, H. Feng, K. Schmidt-Rohr, and H. W. Spiess, Phys. Rev. Lett. **81**, 2727 (1998).
[13] L. Berthier, G. Biroli, J. P. Bouchaud, L. Cipelletti, D. El Masri, D. L'Hote, F. Ladieu, and M. Pierno, Science **310**, 1797 (2005).
[14] C. Dalle-Ferrier, C. Thibierge, C. Alba-Simionesco, L. Berthier, G. Biroli, J. P. Bouchaud, F. Ladieu, D. L'Hote, and G. Tarjus, Phys. Rev. E **76**, 041510 (2007).
[15] S. Capaccioli, G. Ruocco, and F. Zamponi, J. Phys. Chem. B **112**, 10652 (2008).
[16] K. Kessairi, S. Capaccioli, D. Prevosto, M. Lucchesi, and P. A. Rolla, J. Chem. Phys. **127**, 174502 (2007).
[17] J. Ll. Tamarit, M. A. Pérez-Jubindo, and M. R. de la Fuente, J. Phys.: Condens. Matter **9**, 5469 (1997).
[18] W. Huang and R. Richert, J. Chem. Phys. **124**, 164510 (2006).
[19] G. Katana, E. W. Fischer, Th. Hack, V. Abetz, and F. Kremer, Macromolecules **28**, 2714 (1995).
[20] R. Brand, P. Lunkenheimer, and A. Loidl, J. Chem. Phys. **116**, 10386 (2002).
[21] F. Affouard, J. F. Willart, and M. Descamps, J. Non-Cryst. Solids **307–310**, 9 (2002).
[22] K. Kobashi, T. Kyomen, and M. Oguni, J. Phys. Chem. Solids **59**, 667 (1998).
[23] J. F. Willart, M. Descamps, and J. C. van Miltenburg, J. Chem. Phys. **112**, 10992 (2000).
[24] R. Angelini, T. Scopigno, A. Beraud, and G. Ruocco, J. Non-Cryst. Solids **352**, 4552 (2006).
[25] L. Carpentier, R. Decressain, and M. Descamps, J. Chem. Phys. **128**, 024702 (2008).
[26] T. Clark, T. Mc, O. Knox, H. Mackle, and M. A. McKervey, J. Chem. Soc., Faraday Trans. 1 **73**, 1224 (1977).
[27] Y. Huang, D. F. R. Gilson, I. S. Butler, and F. Morin, J. Phys. Chem. **95**, 2151 (1991).
[28] L. A. Fraczyk and Y. Huang, Spectrochim. Acta, Part A **57**, 1061 (2001).
[29] M. Descamps, J. F. Willart, G. Odou, and K. Eichhom, J. Phys. I **2**, 813 (1992).
[30] F. Affouard and M. Descamps, Phys. Rev. B **59**, R9011 (1999).
[31] K. Pathmanathan and G. P. Johari, J. Phys. C **18**, 6535 (1985).

[32] J. P. Amoureux, M. Bee, and J. L. Sauvajol, Mol. Phys. **45**, 709 (1982).
[33] J. P. Amoureux and M. Bee, Acta Crystallogr., Sect. B: Struct. Crystallogr. Cryst. Chem. **35**, 2957 (1979).
[34] J. L. Sauvajol, M. Bee, and J. P. Amoureux, Mol. Phys. **46**, 811 (1982).
[35] G. P. Johari and M. Goldstein, J. Chem. Phys. **53**, 2372 (1970).
[36] O. Yamamuro, M. Ishikawa, I. Kishimoto, J. J. Pinvidic, and T. Matsuo, J. Phys. Soc. Jpn. **68**, 2969 (1999).
[37] J. P. Amoureux, J. L. Sauvajol, and M. Bee, Acta Crystallogr., Sect. A: Cryst. Phys., Diffr., Theor. Gen. Crystallogr. **37**, 97 (1981).
[38] J. Ballon, V. Comparat, and J. Pouxe, Nucl. Instrum. Methods Phys. Res. **217**, 213 (1983).
[39] M. Evain, P. Deniard, A. Jouanneaux, and R. Brec, J. Appl. Crystallogr. **26**, 563 (1993).
[40] Ph. Negrier, J. Ll. Tamarit, M. Barrio, L. C. Pardo, and D. Mondieig, Chem. Phys. **336**, 150 (2007).
[41] L. C. Pardo, M. Barrio, J. Ll. Tamarit, D. O. López, J. Salud, P. Negrier, and D. Mondieig, Phys. Chem. Chem. Phys. **3**, 2644 (2001).
[42] J. J. M. Ramos, Mol. Phys. **90**, 235 (1997).
[43] M. Foulon, J. P. Amoureux, J. L. Sauvajol, J. P. Cavrot, and M. Muller, J. Phys. C **17**, 4213 (1984).
[44] J. P. Amoureux, G. Noyel, M. Foulon, M. Bee, and L. Jorat, Mol. Phys. **52**, 161 (1984).
[45] J. P. Amoureux, M. Castelain, M. D. Benadda, M. Bee, and J. L. Sauvajol, J. Phys. (Paris) **44**, 513 (1983).
[46] M. Tyagi and S. S. N. Murthy, J. Chem. Phys. **114**, 3640 (2001).
[47] M. Descamps, C. Caucheteux, G. Odou, and J. L. Sauvajol, J. Phys. (Paris), Lett. **45**, L719 (1984).
[48] S. A. Lusceac, I. Roggatz, J. Gmeiner, and E. A. Rössler, J. Chem. Phys. **126**, 014701 (2007).
[49] A. Drozd-Rzoska, S. J. Rzoska, S. Pawlus, and J. Ll. Tamarit, Phys. Rev. B **73**, 224205 (2006).
[50] A. Drozd-Rzoska, S. J. Rzoska, S. Pawlus, and J. Ll. Tamarit, Phys. Rev. B **74**, 064201 (2006).
[51] J. P. Amoureux, M. Sahour, C. Fernandez, and P. Bodart, Phys. Status Solidi **143**, 441 (1994).
[52] C. A. Angell, Science **267**, 1924 (1995).
[53] L. C. Pardo, P. Lunkenheimer, and A. Loidl, J. Chem. Phys. **124**, 124911 (2006).
[54] R. Decressain, L. Carpentier, E. Cochin, and M. Descamps, J. Chem. Phys. **122**, 034507 (2005).
[55] M. Foulon, T. Belgrand, C. Gors, and M. More, Acta Crystallogr., Sect. B: Struct. Sci. **45**, 404 (1989).
[56] L. C. Pardo, M. Barrio, J. Ll. Tamarit, D. O López, J. Salud, P. Negrier, and D. Mondieig, J. Phys. Chem. B **105**, 10326 (2001).
[57] A. I. Kitaigorodsky, *Mixed Crystals* (Springer-Verlag, Berlin, 1984).
[58] Cambridge Crytallographic Data Centre, http://www.ccdc.cam.ac.uk/products/csd/radii/.
[59] R. Brand, P. Lunkenheimer, U. Schneider, and A. Loidl, Phys. Rev. Lett. **82**, 1951 (1999).
[60] J. Kirkwood, J. Chem. Phys. **7**, 911 (1939); H. Frölich and H. Frohilich, *Theory of Dielectrics* (Oxford University Press, London, 1949).
[61] R. J. Sengwa and S. Sankhla, J. Mol. Liq. **130**, 119 (2007).
[62] G. Parthipan and T. Thenappan, J. Solution Chem. **36**, 1231 (2007).
[63] A. C. Kumbharkhane, S. M. Puranik, and S. C. Mehrotra, J. Solution Chem. **22**, 219 (1993).
[64] S. J. Suresh and V. M. Naik, J. Chem. Phys. **116**, 4212 (2002).
[65] V. P. Pawar and S. C. Mehrotra, J. Mol. Liq. **115**, 17 (2004).
[66] V. P. Pawar, A. R. Patilb, and S. C. Mehrotra, J. Mol. Liq. **121**, 88 (2005).
[67] M. Valiskó, D. Boda, J. Liszi, and I. Szalai, Phys. Chem. Chem. Phys. **3**, 2995 (2001).
[68] C. A. Angell, J. Non-Cryst. Solids **131–133**, 13 (1991).
[69] R. Böhmer, K. L. Ngai, C. A. Angell, and D. J. Plazek, J. Chem. Phys. **99**, 4201 (1993).
[70] C. A. Angell, Polymer **38**, 6261 (1997).
[71] G. Tarjus, S. A. Kivelson, Z. Nussinov, and P. Viot, J. Phys.: Condens. Matter **17**, R1143 (2005).
[72] R. Kohlrausch, Ann. Phys. Chem. **91**, 179 (1854).
[73] G. Williams and D. C. Watts, Trans. Faraday Soc. **66**, 80 (1970).
[74] A. Alegría, E. Guerrica-Echevarría, L. Goitiandía, L. Lellería, and J. Colmenero, Macromolecules **28**, 1516 (1995).
[75] S. Capaccioli and K. L. Ngai, J. Phys. Chem. B **109**, 9727 (2005).